JOURNAL OF APPLIED ELECTROCHEMISTRY 4 (1974) 91–108

REVIEW

The rotating cylinder electrode

D. R. GABE*

Department of Metallurgy, University of Sheffield, U.K.

Received 12 November 1973; revised MS received 4 December 1973.

Contents

1. Introduction
2. Design and construction of the RCE
3. Fluid behaviour in the rotating cylinder cell
   3.1. Inner rotating cylinder
   3.2. Outer rotating cylinder
4. Mass transport at the RCE
   4.1. Empirical data
   4.2. Dimensionless group analysis
   4.3. Theoretical analysis
5. Applications of the RCE
   5.1. Electroanalysis
   5.2. Electrodeposition
   5.3. Cementation
   5.4. Corrosion and dissolution

References

Glossary of symbols

b	Constant
C_s, C_b	Surface and bulk concentrations
D	Diffusion coefficient
d	Characteristic dimension
zF	Faradaic equivalence
F	Shear force
f	Friction factor
I_d	(Diffusion) current
i_L	(Limiting) current density
J	Mass flux (see Equation 24)
K	Constant
L, l	Length of cylinder
Δl	Gap between cylinder and cell bottom
M	Segment length
n	Index, integer
R_1, R_2	Radii of inner and outer cylinders
r	Radial distance
r_o/K_s	RDE roughness factor (see Equation 4)
T	Torque
U	Peripheral velocity ($= \omega R$)
X	Parameter of convenience
y	Distance
α	Densification coefficient
β	Velocity gradient or profile
δ, δ_o	Thickness of Nernst diffusion and Prandtl hydrodynamic boundary layers
ε	Roughness dimension (see Equation 27)
η	Coefficient of viscosity
ρ	Density
ν ($= \eta/\rho$)	Kinematic viscosity
τ	Shear stress
χ	Roughness factor (see equation 34)
ω	Angular velocity
Re	Reynolds number, usually defined as $\mathrm{Re} = (R_i U/\nu)$
Sc	Schmidt number $= \nu/D$
Sh	Sherwood number $= J R_1/DC_b$
St	Stanton number $= J/U C_b$
Gr	Grashof number $= (C d^3 \alpha g)/\nu^2$
Ta	Taylor number (see Equation 22)
Pe	Peclet number $= \beta L^2/2D$

1. Introduction

In the measurement of kinetic parameters for electrochemical reactions one of the problems of steady state rather than transient conditions is to eliminate random effects of free convection in the electrolyte. Such free convection develops by virtue of changes in temperature and density of solution at the electrode/electrolyte interface and can in principle be expressed, described and analysed often in terms of the Grashof number, Gr. However its elimination, or rather its

*Present address: Department of Materials Technology, University of Technology, Loughborough, U.K.

neglect relative to superimposed forced convection, is relatively easy and commonplace. The most widely used technique is to use a Rotating Disc Electrode (RDE) in which the electrode surface is circular and rotated in a horizontal plane at speeds from 100–5000 r.p.m.; practical aspects are now well-known [1, 2] and the hydrodynamics reasonably well understood [3, 4]. The particular virtue of the RDE is that laminar or streamlined flow is maintained over a very wide range of rotation speeds and the transition to turbulent flow occurs at Reynolds numbers $10^4 < Re_{crit} < 10^5$. In laminar flow the thickness of the diffusion layer is constant over the whole area of the disc and the concentration distribution is stationary except at the edge (the ring disc eliminates this particular error). In laminar flow the limiting current density is given by:

$$i_L = 0{\cdot}62\, zFC_0D\left(\frac{\nu}{D}\right)^{\frac{1}{3}}\left(\frac{\omega}{\nu}\right)^{\frac{1}{2}} \quad (1)$$

or in terms of dimensionless groups:

$$Sh = 0{\cdot}62\, Re^{\frac{1}{2}}Sc^{\frac{1}{3}} \quad (2)$$

The direct relation between limiting current density and ω, D and C makes it very convenient to use. For turbulent flow the relationships are not so clear but an approximate relationship would be:

$$Sh \simeq 0{\cdot}01\, Re^{0{\cdot}9}\, Sc^{0{\cdot}25} \quad (3)$$

A more exact relation has been given by Cornet *et al.* [5]:

$$Sh = Sh_c\frac{Re_c}{Re} + 0{\cdot}02\, ReSc^{\frac{1}{3}}\left(\frac{\tau_0}{K_s}\right)^{-0{\cdot}272}\left(1-\frac{Re_c}{Re}\right)$$

$$\simeq 0{\cdot}0198\, Re^{0{\cdot}8}\, Sc^{0{\cdot}33} \quad (4)$$

Where subscript c refers to the critical transition value and (r_0/K) is a roughness factor.

The Rotating Cylinder Electrode (RCE) has been relatively little used in analytical chemistry —a field in which the RDE is widely used—but has found some application elsewhere.

For this electrode, reaction rates may again be mass transport controlled, and provided the IR drop is constant in the cell the current distribution over the electrode surface may be uniform and concentration changes may be calculated even though the fluid flow is generally turbulent. Cases of laminar flow are strictly limited because in the conventional arrangement the RCE is enclosed within a concentric cell and $Re_{crit} \simeq 200$ corresponding to rotation speeds of <10 r.p.m. A higher critical Reynolds number results when the outer cylinder is rotated but this may create difficulties in construction and so is little used. Notwithstanding the supposed instability of turbulent motion, the RCE has found a wide variety of applications especially when naturally turbulent industrial processes have to be simulated on a smaller scale or when mass transport must be maximized. Such applications embrace electrodeposition, corrosion and dissolution, cementation, etc. By contrast the RDE is most usefully employed when laminar flow regimes must prevail for stability.

The mass transport relation for the RCE is less well understood than for the RDE. Early workers made use of rotating rods or wires and found that $i_L = kU^n$ where n varied from 0·5 to 0·9, this wide range being attributed to variations in the degree of turbulence, geometry of the cell and roughness factors, partial reaction control and gas evolution as a secondary reaction. Dimensionless group correlation was first achieved by Eisenberg *et al.* [6, 7] for turbulent flow and this has been found to describe many other similar situations.

$$i_L = 0{\cdot}0791\, zFC_bU^{0{\cdot}7}\left(\frac{R_1}{\nu}\right)^{-0{\cdot}3}\left(\frac{\nu}{D}\right)^{-0{\cdot}644} \quad (5)$$

or

$$Sh = 0{\cdot}0791\, Re^{0{\cdot}7}\, Sc^{0{\cdot}356} \quad (6)$$

An alternative form uses the Stanton number, St

$$St = 0{\cdot}0791\, Re^{-0{\cdot}3}\, Sc^{-0{\cdot}644} \quad (7)$$

Taking a velocity dependence of the form $i_L = kU^n$ it may be seen that in turbulent flow n is 0·67–0·70 while for laminar flow n is 0·33 and the correlation rather more complicated.

Much basic theory for the behaviour of fluids in concentric cylinder cells has been obtained from studies in other fields such as heat transfer [8] and fluid dynamic stability [9]; in particular the use of concentric rotating cylinders as a viscometer for the measurement of viscosity for either gases or liquids [10, 11].

While the electrochemical method is a very convenient means of continuously measuring mass transport (flux $J = i_L/zF$), there are severe limitations placed on the choice of electrode reaction [12]. The following criteria must be applied

(i) The reaction is diffusion-controlled.
(ii) The reaction is stoichiometric and the number of electrons, n, achieving discharge is known and constant.
(iii) The current efficiency is 100%.
(iv) A limiting current density can be clearly read from a potential-current density polarization graph.

In practice simple reactions taking place at electrode potentials of $0 \pm 0{\cdot}4$ V (H-scale) are used to avoid gas evolution and amongst the most popular are the ferrocyanide/ferricyanide redox reaction and cathodic deposition of copper from sulphate-sulphuric acid solutions. Anodic dissolution has been found to be hazardous as reaction rather than diffusion may become rate-controlling and more base metals than copper may have hydrogen co-discharged. Chemical dissolution and cementation have also been used but here the electrochemical advantages may be lost.

The technique may be used to discriminate between charge transfer and mass transfer controlled reactions and the contributions of each towards total overpotential [13] but this should be limited to reactions which are known to satisfy all common criteria.

2. Design and construction of the RCE

Many of the early designs paid little or no attention to the fluid dynamics of rotation and were primarily concerned with achieving a particular rotation speed. For example, Brunner [14] used an electrode capable of being rotated at 150 r.p.m. while Bennett [15] was able to achieve 6000 r.p.m. while supplying 300 A to the electrode surface (3500 A ft^{-2}). Other similar investigations may be found in the literature [16–18] none of which consider the fluid dynamics and few of which describe the cell in sufficient detail to enable subsequent investigators to deduce any detailed characteristic. Furthermore, although Swalheim [19] made an important contribution in both design and application it was not until Eisenberg *et al.* [6, 7] investigated the effects of cell geometry that any full understanding of the RCE could be claimed.

Design of the RCE necessarily has several features in common with the RDE because it is essential to be able to rotate the electrode at both low and high speeds—ideally continuously variable over the whole range—and to be able to measure that speed and maintain it constant. Design of the bearings is important to ensure smooth rotation and to enable centring adjustments to be made to eliminate eccentricity and 'whip' in rotation. Means of supplying electrical power to the electrode with minimum contact resistance must be devised and in some applications must be capable of handling up to 500A Design of the cell may also be of importance although this is usually governed by electrical and electrochemical considerations rather than those of fluid dynamics.

The most detailed descriptions of apparatus have been given by Swalheim [19] and Eisenberg *et al.* [6, 7], but more recent innovations may be found in many papers [12, 20–25]. Swalheim [19] constructed many of his components from bakelite and Eisenberg *et al.* [6, 7] from lucite; present practice would make use of perspex for the cell and stainless steel for the rotor and cylinder/former. Eisenberg *et al.* [6, 7] showed that the cylindrical electrode itself could be machined from blocks of chemicals such as benzoic or cinnamic acid thereby enabling chemical dissolution experiments to be made. The cylinder geometry is usually defined in terms of the length to diameter ($l/2R_1$) ratio which Eisenberg *et al.* [6, 7] varied from 3·0 to 0·3 although most investigations have used a fixed geometry. Both low [26, 27] and high [19, 21] ratios have been favoured but Robinson and Gabe [23] have pointed out the advantages of taking a high ratio cylinder but using only a portion of active area and hence lower ratio. Rotation speed is measured most simply with a tachometer [6, 7 19] but a more sensitive device would be a stroboscope or an electronic e.m.f. tachometer [23, 24] or counter [25].

Conventionally power may be supplied through metal spring brushes [19] although for

continuous high speed use effects of fretting damage may cause increasing electrical resistance to develop (Fig. 1). Carbon brushes [22, 25] have speeds [6, 7, 12, 21, 24] but at higher speeds (>1300 r.p.m.) the mercury may produce its own vortex or spray causing poor contact [24]. There

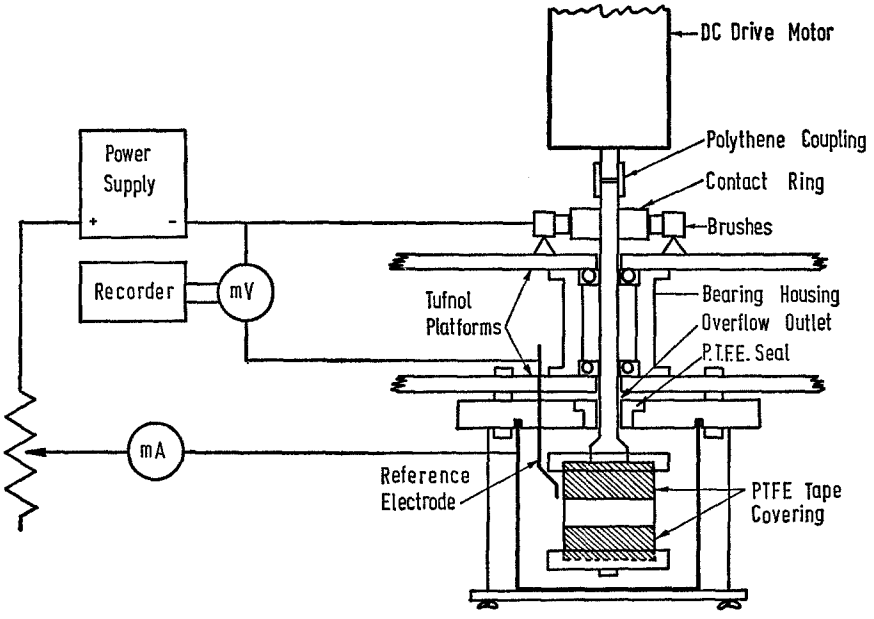

Fig. 1. Rotating cylinder cell having ratio $R_1/L \doteq 1$ and incorporating carbon brush contacts. (*After* Robinson and Gabe.)

the advantage of yielding conducting, lubricating fretting products and the brush is slowly 'machined' to a precise fit on the contact rotor collar but for high current applications silver impregnated graphite brushes acting on a silver plated contact collar have been found to be most satisfactory [23, 24]. The use of a mercury contact well has been advocated and found to be most satisfactory for relatively low rotation is the additional hazard of liquid metal stress corrosion by the mercury on the well metal (Fig. 2).

Swalheim [19] placed considerable emphasis on the design of the cell to contain the RCE and in particular used vertical baffles to break up vortices and ensure completely turbulent flow. Subsequently Eisenberg *et al.* [6, 7] showed, by varying the cell sizes and thereby the gap width,

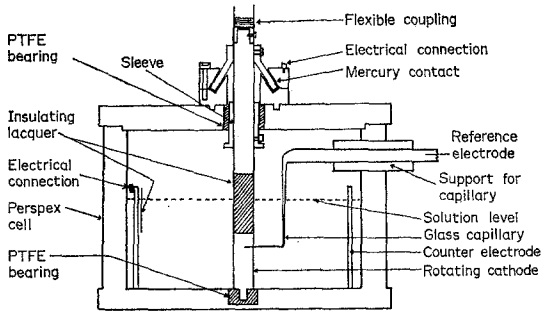

Fig. 2. Rotating cylinder cell having ratio $R_1/L < 1$ and incorporating mercury well contacts. (*After* Edwards and Wall.)

that the cell design has relatively little influence on the fluid behaviour because the onset of turbulence depends upon a Reynolds number defined by the diameter of the rotating cylinder. The critical value of Re is quite low (100–200) and the influence of baffles in the cell may well be insignificant. If the electrode gap is significant in any way it is only so in electrochemical terms. The power consumption of the cell may be primarily dependent upon the voltage drop across the electrolyte within the gap which is therefore minimized to reduce power losses and heating effects. The baffles would be useful if the electrode was used in the laminar regime when it would stop the fluid gaining its own momentum and thereby rotating with the inner cylinder.

Analogous design considerations apply to the concentric cylinder cells used in viscometry but in this case rotation speeds are low and within the laminar flow regimes and electrical contact problems are absent and insufficient time is allowed for the fluid to gain its own rotational momentum. Details of construction of such a cell may be found in the literature [28].

Details of design may be influenced by the type of application envisaged. One such case is highlighted by the considerations of Swalheim [19], and later Beard *et al.* [22], who were intent upon devising a laboratory cell to simulate high speed plating of strip. For this purpose a strip substrate was wrapped around the cylinder, acting as former, which could subsequently be removed for further treatment or microscopic examination. Others, notably Dimon, Thwaites and Barry [29–31], have argued that a circulating electrolyte cell in which the cathode is incorporated as a planar sheet is better because the substrate need not be flexed in any way on its removal from the cell. The circulating cell certainly does have advantages if variables of electrolyte composition are being examined but unfortunately the onset of turbulence takes place at much higher values of Re than for the RCE and it has been argued that this and other reasons makes the RCE a more satisfactory simulation of a continuous tinplate process [32]. The need to simulate natural convection and low rates of forced convection in electrolytic refineries is another field in which the RCE may prove useful but it is not yet clear how the true pattern of flow in a refinery can be satisfactorily expressed [33–35].

3. Fluid behaviour in the rotating cylinder cell

The viscosity of a fluid is related to the shear stress required to cause shear between adjacent layers of a moving fluid and the velocity gradient across the interface of those layers by Newton's law:

$$\tau = \eta \frac{dU}{dy} \tag{8}$$

where η is the coefficient of viscosity having typical units of g ms^{-1} (N.B. the kinematic viscosity ν is the ratio of η/ρ where ρ is the density). Not only does Newton's law indicate a means of measuring viscosity but it indicates the simplest way of expressing the velocity gradient or profile of a moving fluid. That it is simple is clear when we examine motion in the concentric cylinder cell. Taking the case of a rotating inner cylinder (radius R_1 angular velocity ω) and a static outer cylinder (radius R_2, angular velocity $\omega_2 = 0$) the velocity profiles for laminar and turbulent flow may be as shown in Fig. 3. The laminar flow profile is often expressed as a para-

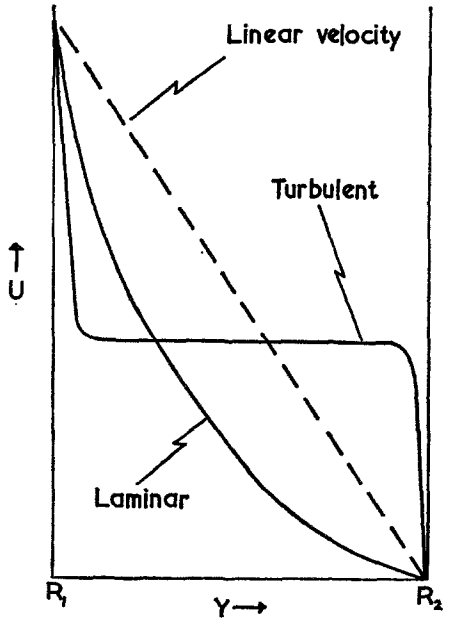

Fig. 3. Velocity profiles in a rotating cylinder cell (inner cylinder radius R_1 rotates).

bolic relationship but the turbulent profile must take a more complicated form. For example:

$$\text{laminar flow } U = \text{const}\,\frac{y^2}{(R_2-R_1)^2} \tag{9}$$

$$\text{turbulent flow } \frac{U}{(\tau_0/\rho)^{\frac{1}{2}}} = \text{const}\log\frac{y}{(R_2-R_1)} \tag{10}$$

Clearly a linear profile, as is used in Newton's law for adjacent shearing layers, is a gross approximation for the whole gap yet may be appropriate for specific regions of that gap.

In considering fluid behaviour within the cylindrical annulus we may examine two cases. Firstly, the case of a stationary outer cylinder and rotating inner cylinder which is most widely used for mass transfer studies and which is the basis of the Stormer-type viscometer, and secondly the case of a stationary inner cylinder and rotating outer cylinder which is less widely used except as a McMichael-type viscometer. Behaviour is essentially similar but the two cases will be examined separately making different assumptions concerning the velocity profile.

3.1. *Inner rotating cylinder*

If we consider an elemental cylinder of liquid at radius r and thickness δr an angular velocity ω_r will be imparted to that layer by the inner rotating cylinder. Assuming a linear angular velocity gradient ($d\omega_r/dr$) the true velocity gradient across the elemental cylinder will be (see Fig. 4):

$$\frac{dU_r}{dr} = \frac{d(\omega_r r)}{dr} = r\frac{d\omega_r}{dr} + \omega \tag{11}$$

Then from Newton's law the shearing force across the elemental cylinder of length l is:

$$F = -2\pi\, rl\eta\left(r\frac{d\omega_r}{dr}\right) \tag{12}$$

The force is negative because the angular velocity decreases such that $\omega = 0$ at $r = R_2$. Therefore, the torque inducing the rotational

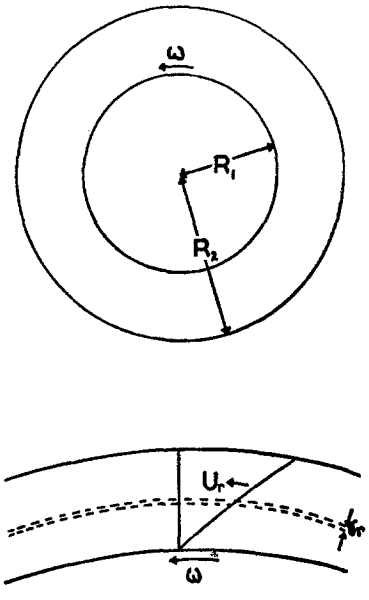

Fig. 4. Fluid motion for a cell in which the inner cylinder rotates.

motion on the cylinder at radius r is

$$T = Fr = -2\pi\eta l r^3\left(\frac{d\omega_r}{dr}\right) \tag{13}$$

The torque applied to the inner cylinder to produce this rotational motion over the whole gap (R_2-R_1) can be found as

$$-T\int_{R_1}^{R_2}\frac{dr}{r^3} = 2\pi\eta l\int_{\omega}^{0} d\omega_r$$

$$\frac{T}{2}\left[\frac{1}{R_1^2}-\frac{1}{R_2^2}\right] = 2\pi\eta l\omega$$

Hence

$$T = 4\pi\eta l\omega\Big/\left(\frac{1}{R_1^2}-\frac{1}{R_2^2}\right) \tag{14}$$

or

$$\omega = \frac{T}{4\pi\eta l}\left(\frac{R_2^2-R_1^2}{R_1^2R_2^2}\right) \tag{15}$$

3.2. *Outer rotating cylinder*

If we take the case of the outer cylinder rotating at angular velocity ω the velocity U_r at radius r

(Fig. 5) can be expressed as:

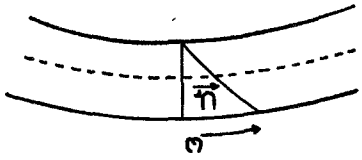

Fig. 5. Fluid motion for a cell in which the outer cylinder rotates.

$$U_r = \frac{\omega R_2\left[\frac{R_1}{r} - \frac{r}{R_1}\right]}{\left[\frac{R_1}{R_2} - \frac{R_2}{R_1}\right]} \tag{16}$$

The shear stress distribution is given by

$$\tau_r = -\eta r \frac{d}{dr}\left[\frac{\omega R_2}{r}\frac{\left(\frac{R_1}{r} - \frac{r}{R_1}\right)}{\left(\frac{R_1}{R_2} - \frac{R_2}{R_1}\right)}\right]$$

$$\tau_r = -2\eta\omega R_2^2 . \frac{1}{r^2}\left[\frac{(R_1/R_2)^2}{1-\left(\frac{R_1}{R_2}\right)^2}\right] \tag{17}$$

The torque T at $r = R_2$ is given by:

$$T = 2\pi R_2 l \tau R_2$$

$$= -4\pi\eta l\omega\left(\frac{R_1^2 R_2^2}{R_2^2 - R_1^2}\right) \tag{18}$$

Here the negative sign indicates a negative velocity gradient otherwise the equation is as before.

However, both of these approaches disregard the torque on the submerged end of the cylinder. If this 'end correction' is to be determined experimentally by a calibration technique the end disc of the cylinder may be regarded as having an equivalent length L so that the total length of cylinder is effectively $(l+L)$. Alternatively, if the clearance between end disc and cell bottom is Δl then the torque due to the disc is

$$T_1 = \frac{\eta\omega\pi R_1^4}{2\Delta l} \tag{19}$$

and the total torque is

$$\sum T = \eta\omega\pi R_1^2\left[\frac{4l R_2^2}{(R_2^2 - R_1^2)} + \frac{R_1^2}{2\Delta l}\right] \tag{20}$$

When the rotating cylinder cell is used as a viscometer one cylinder is rotated at constant velocity and the torque transmitted to the other cylinder through the fluid is measured as the rotation in a calibrated torsion fibre/spring or as the time taken for the cylinder to rotate through 360°. Sufficiently high rotation speeds are used to make the effect of bearing friction negligible yet slow enough to ensure laminar flow in the fluid.

The onset of turbulent flow takes place at a critical value of Reynolds number Re*. An early consideration of Re* was given by Mallock [36] who gave its value as 1900 when Re was defined as:

$$\mathrm{Re} = \frac{\omega(R_2^2 - R_1 R_2)\rho}{\eta} \tag{21}$$

In this definition it is assumed that the outer cylinder rotates with peripheral velocity $U = \omega R_2$ in which case the critical dimension employed is the gap width $(R_2 - R_1)$. The viscosity term is more usually the kinematic viscosity $\nu\ (= \eta/\rho)$.

The case of an inner cylinder rotating has been considered by Taylor [37–39] and subsequently by Lin [40] and Flower *et al.* [41] who showed that instability occurs when the Taylor number Ta = 29·3 where

$$\mathrm{Ta} = \mathrm{Re}\left(\frac{R_2 - R_1}{R_2 + R_1}\right)^{\frac{1}{2}},\ \mathrm{Ta}^* = 29{\cdot}3 \tag{22}$$

and

$$\mathrm{Re} = \frac{R\omega(R_{12} - R_1)}{\nu} \tag{21a}$$

An alternative expression for the critical angular velocity ω^* was:

$$\omega^* = \frac{\pi^2\nu(R_1 + R_2)}{2JR_1^2(R_2 - R_1)} \tag{23}$$

where

$$J = 0{\cdot}0571\left[1-0{\cdot}652\left(\frac{R_2-R_1}{R_1}\right)\right] + 0{\cdot}00056\left[1-0{\cdot}652\left(\frac{R_2-R_1}{R_1}\right)\right]^{-1} \quad (24)$$

However, once again the critical dimension is taken to be the gap (R_2-R_1) although it is now believed that the critical dimension ought to be R_1—see the dimensionless group analysis. Schlichting [42] has defined a modified Taylor number Ta^1 as follows:

$$Ta^1 = Re\left(\frac{R_2-R_1}{R_1}\right)^{\frac{1}{2}} \quad (22a)$$

and using this definition the critical value is $Ta^1 = 41{\cdot}3$. Below this value normal laminar flow exists while immediately above this value Taylor vortices develop; these are illustrated in Fig. 6 and may be described as cellular or

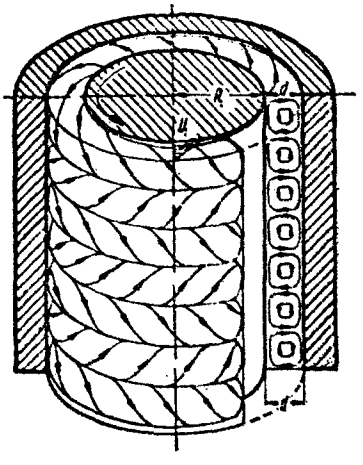

Fig. 6. Schematic diagram of the toroidal Taylor vortices. (*After* Schlichting.)

toroidal vortices within an essentially laminar regime. For $Ta > 400$ true turbulent flow develops.

This uncertainty of definition may well be part of the reason why Jerrard [43] found it difficult to formulate a criterion similar to that of Taylor for the rotating outer cylinder and has suggested that a set of tables rather than a formula gives a better formulation. With a rotating outer cylinder centrifugal forces stabilize the laminar flow regime and the value of Re* is usually much higher than for the case of the rotating inner cylinder where turbulence commences at $Re > 200$ as three-dimensional laminar vortices develop [37]. It is also important to appreciate that the Taylor analysis is strictly restricted to the case when $(R_2-R_1) \ll \frac{1}{2}(R_1+R_2)$ and the case for large annular gaps has been discussed by Chandrasekhar [44].

Newman [4] considers that we ought to define three regimes of behaviour. First at low rotation speeds the laminar regime where flow is tangential; secondly, at a transition defined by the Taylor number and

$$Re = U(R_2-R_1)/\nu$$

where flow remains laminar but no longer tangential as Taylor vortices develop giving a superimposed radial and axial motion. Thirdly, at a transition defined by

$$Re = UR_1/\nu,$$

true turbulence develops and it is here that rates of mass transport are markedly increased.

The laminar-turbulent transition may be illustrated graphically [39] as in Fig. 7 which

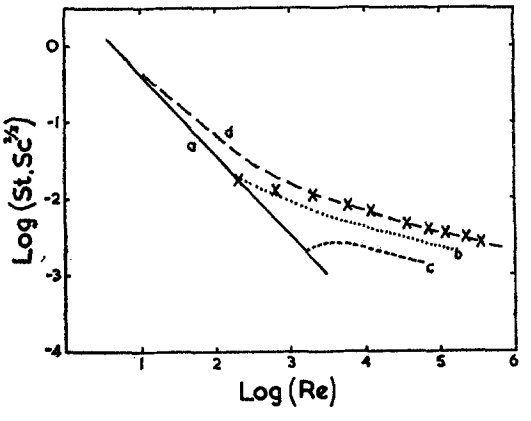

Fig. 7. The laminar-turbulent transition. Compendium of data:
(a) Laminar flow [39]
(b) Turbulent flow, inner cylinder rotated [39]
(c) Turbulent flow, outer cylinder rotated [39]
(d) Experimental line, inner cylinder rotated [45]
× × Experimental points, inner cylinder rotated [6, 7].

includes the time for laminar flow (essentially Poiseuille behaviour) and times for turbulent flow when the inner and outer cylinders rotate. The experimental data of Theodorsen and

Regier [45] suggest that the transition is not sharp (although other factors such as roughness could be important) and also showed that the critical dimension was the cylinder diameter and not the annular gap as proposed by Taylor. Donnelly and co-workers in a series of papers [46] have examined the stability of viscous flow in the torsional cylinder cell and their graph of torque against angular velocity shows a large transition region which again provides evidence of the discreet region where Taylor vortices are stable.

Theodorsen and Regier [45] also measured drag coefficients on inner rotating cylinders in various fluids and correlated them with Re by means of the friction factor f:

$$\log \mathrm{Re} = 0{\cdot}1737\left(\frac{f}{2}\right)^{-\frac{1}{2}} - \log\left(\frac{f}{2}\right)^{\frac{1}{2}} + 0{\cdot}2979 \tag{25}$$

or in an alternative form:

$$\left(\frac{f}{2}\right)^{-\frac{1}{2}} = -17{\cdot}5 + 5{\cdot}75 \log\left[\mathrm{Re}\left(\frac{f}{2}\right)^{\frac{1}{2}}\right] \tag{25a}$$

This equation has been applied in several different ways. Eisenberg *et al.* [6, 7] showed that in the turbulent regime $10^3 < \mathrm{Re} < 10^5$ the relation can be approximated to:

$$\frac{f}{2} \simeq 0{\cdot}0794\ \mathrm{Re}^{-0{\cdot}30} \tag{26}$$

and utilized this in the justification of their dimensionless group analysis. Makrides and Hackerman [47] and Kappesser *et al.* [25] have considered the way in which micro-roughness of the rotating surface may affect roughness, especially when the roughness increases as dissolution proceeds, and show that by incorporating a roughness dimension ε the friction factor becomes:

$$\left(\frac{f}{2}\right)^{-\frac{1}{2}} = 1{\cdot}25 + 5{\cdot}76 \log\left(\frac{R_1}{\varepsilon}\right) \tag{27}$$

4. Mass transport at the RCE

4.1. *Empirical data*

Much of the earliest work in the field of rotating electrodes—whether anodes or cathodes—was arbitrary and empirical and the more practical aspects have been reviewed elsewhere [18]. Only a few investigators made any attempt to obtain quantitative relationships between rotation speed and the limiting current density and in many cases the cell geometry was sufficiently peculiar to make the result unique. Brunner [14] and Nernst and Merriam [48] and others [49–51] showed that for the relationship $i_L = kU^n$ the index n had a value of 0·67–0·70 although van Name and Edgar [52] suggested that a value as high as 0·9 might be obtained. In general these investigators used relatively low rotation speeds (0–600 r.p.m.) although Bennett [15] reported using pipes as cathodes at speeds of up to 6000 r.p.m. Eucken [53, 54] rotated the outer cylinder using a planar inner electrode and found $n = 0{\cdot}5$ but this is clearly a special case. Many other investigators used the technique to examine the properties of electrodeposits without examining the effect of rotation speed quantitatively [16–18, 55] but anomalies were very evident from studies of anodic dissolution. Roald and Beck [56] showed that for the dissolution of magnesium in hydrochloric acid $n = 0{\cdot}71$ but at higher acid concentrations the rate was independent of rotation speed. This they attributed to bubbles of hydrogen causing *additional* agitation and King [57] examined quantitatively the agitative effect of bubble evolution. Earlier work by King and co-workers [58–64] showed that at low rotation speeds $n = 0{\cdot}7$ but as the rotation rate increased to above about 1000 r.p.m. the value of $n \to 1$ and in some cases no correlation was apparent [61]. Concurrent work by King *et al.* on cementation at rotating rods [65–67] and later work on corrosion and dissolution [68, 69] showed that at high rotation speeds chemical reaction rather than mass transport becomes rate-controlling and so dissolution becomes independent of speed. For a particular displacement reaction by zinc [70] the reaction rate was found to be proportional to velocity within the low range of 50–400 r.p.m. and above this speed they were independent and Ingraham *et al.* [71–73] have shown that the transition values clearly depend upon the particular reaction involved. In general the correlation of Eisenberg *et al.* [6, 7] is obeyed at low speeds

within the turbulent flow regime although some occasional dissidence may be noted [74–76].

The effects of cell geometry, e.g. cylinder diameter, inter-cylinder gap, length/radius ratio, etc., have been investigated on several occasions [6, 7, 47, 61] and within certain limits can be neglected in practice. However, Makrides and King and Cornet *et al.* [25, 47, 69, 77] have examined the effects of surface roughness on dissolution in the critical ranges of rotation speed and have attempted to express the effect quantitatively.

4.2. *Dimensionless group analysis*

The relevance of so many variables makes it obvious that the most convenient way of handling the experimental data is by means of dimensionless groups. For the RCE, four such groups have been used:

(a) Reynolds number, Re, defining relative flow velocity in terms of the critical dimension.
(b) Schmidt number, Sc, defining the transport properties of the fluid.
(c) Sherwood number, Sh, a mass transfer coefficient.
(d) Stanton number, St, a velocity dependent mass transfer coefficient.

The first systematic correlation making use of all the measured parameters U, d, ν $(=\eta/\rho)$, C, D and i_L was deduced by Eisenberg *et al.* [6] who showed [7] (see Fig. 8) that the critical dimension d was in fact the diameter of the rotating cylinder R_1 rather than the gap (R_2-R_1). They obtained for the ferri-ferrocyanide redox reaction:

$$i_L = 0{\cdot}0791\ zFCU^{0{\cdot}7}d^{-0{\cdot}3}\nu^{-0{\cdot}344}D^{0{\cdot}644} \quad (28)$$

which expressed in terms of dimensionless numbers is either:

$$\mathrm{St} = 0{\cdot}0791\ \mathrm{Re}^{-0{\cdot}3}\ \mathrm{Sc}^{-0{\cdot}644} \quad (29)$$

or

$$\mathrm{Sh} = 0{\cdot}0791\ \mathrm{Re}^{0{\cdot}7}\ \ \mathrm{Sc}^{0{\cdot}356} \quad (30)$$

For the case of a static inner cylinder and rotating outer cylinder Arvia and Carrozza [20]

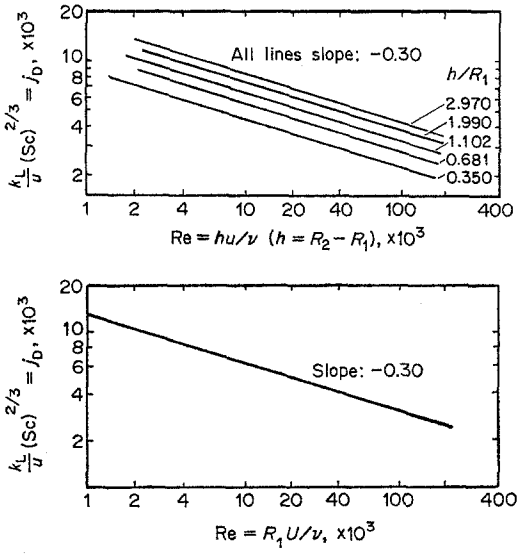

Fig. 8. Mass transport correlation assuming: (Top) $\mathrm{Re} = \frac{(R_2-R_1)\,U}{\nu}$; (Below) $\mathrm{Re} = \frac{R_1\,U}{\nu}$ (*After* Eisenberg *et al.* [7].)

found for one solution (i.e. constant Sc):

$$J = 0{\cdot}0791\ \mathrm{Re}^{-0{\cdot}3}\left(\frac{R_1}{R_2}\right)^{-0{\cdot}70} \quad (31)$$

but this has found relatively little further application [53, 78].

The relationship of Eisenberg *et al.* [6, 7] was effectively confirmed by Robinson and Gabe [23, 24, 79] who obtained for the cathodic electrodeposition of copper from $CuSO_4$-H_2SO_4 solutions (see Fig. 9):

$$\mathrm{St} = 0{\cdot}0791\ \mathrm{Re}^{-0{\cdot}31}\ \mathrm{Sc}^{-0{\cdot}59} \quad (32$$

They subsequently pointed out [80] that critical review of the literature reveals some slight variation in the values of the power indices; for example the indice for Re has been reported as −0·30 [6, 7, 20], −0·31 [79], −0·333 [81] and −0·40 [82], while for Sc indice values reported include −0·59 [79], −0·644 [6, 7, 20, 83] and −0·666 [82]. Others have confirmed the relation without extensive investigation [84, 85].

Newman [4, 86] has pointed out that the ratio of inner to outer cylinder diameters should be incorporated in the correlation and implies that

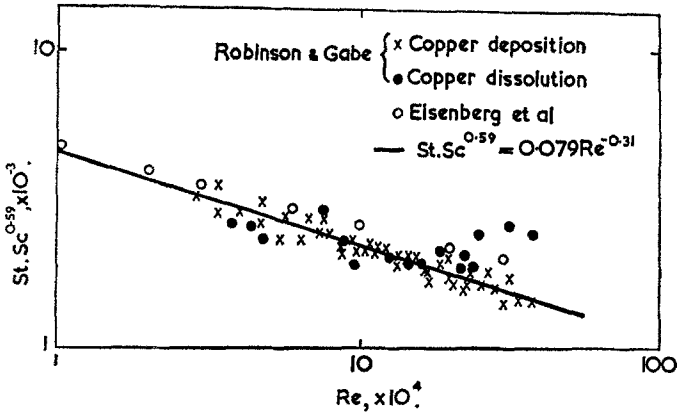

Fig. 9. Mass transport correlation incorporating data for copper deposition [6, 7, 23, 24] and copper dissolution [24].

its effect is really on modifying Re:

$$\mathrm{Sh} = 0{\cdot}0791\left[\mathrm{Re}\left(\frac{R_1}{R_2}\right)\right]^{0{\cdot}7}\mathrm{Sc}^{0{\cdot}356} \qquad (33)$$

In practice $R_1/R_2 \simeq 1$ and $(R_1/R_2)^{0{\cdot}7} \to 1$; any departure from this value may be noticed as a change in the constant. More important is the possible effect of surface roughness on the correlation—this affects the friction factor which is the main variable influencing the constant. Makrides and Hackerman [47, 77] found that, for the relation $i_L = K\,U^n$, n had values of 0·72–0·77, not 0·70 as reported by Eisenberg *et al.* [6, 7] although in fact the l/d ratios for their cylindrical electrodes were very different—l/R_1 of 1·0–1·2 compared with l/R_1 of 3–11·6 for Eisenberg *et al.* More important, however, a mass transport equation including a roughness factor was proposed:

$$i_L = zFC\left[1{\cdot}25+5{\cdot}76\log\left(\frac{R_1}{\chi}\right)\right]^{-2}\left(\frac{\nu}{D}\right)^{-0{\cdot}644}U \qquad (34)$$

Where χ is the average roughness 'height'. Kappesser *et al.* [25] have subsequently confirmed this relation for a wide range of surface roughness preferring, however, to express it as:

$$\mathrm{Sh} = \left(\frac{f}{2}\right)\mathrm{Re}\,\mathrm{Sc}^{0{\cdot}356} \qquad (35)$$

where

$$\frac{f}{2} = \left[1{\cdot}25+5{\cdot}76\log\left(\frac{R_1}{\chi}\right)\right]^{-2} \qquad (36)$$

In these relationships $i_L = K\,U$. It is believed that although obtained in anodic dissolution experiments it is not due to reaction rate control but rather to roughening of the electrode surface as dissolution takes place.

These results described above cover the vast range of rotation velocities encountered in practice and which are within the turbulent regime. However, at very low rotation speeds (<10 r.p.m.) laminar flow is possible. Relatively little interest in this region exists; nevertheless, Cornet and Kappesser [81] have examined behaviour at the critical value of Re (≃200) and found for one solution (i.e. constant value of Sc):

Re<200	Sh = 37
Re>200	Sh = 0·97 $\mathrm{Re}^{0{\cdot}64}$

The transition is illustrated in Fig. 10.

In the laminar regime the value of 37 was attributed to the fact that the relation is in fact:

$$\mathrm{Sh} = f\,\mathrm{Re}\,\mathrm{Sc}^{\frac{1}{3}} \qquad (37)$$

but that in this particular case f = constant/Re and Sc ≃ 460. Making a similar assumption about Sc in the relation for turbulent flow their equation is not dissimilar to the relation of Eisenberg *et al.* [6, 7].

Independent data for the laminar region are sparse. Kambara *et al.* [87] in a series of papers

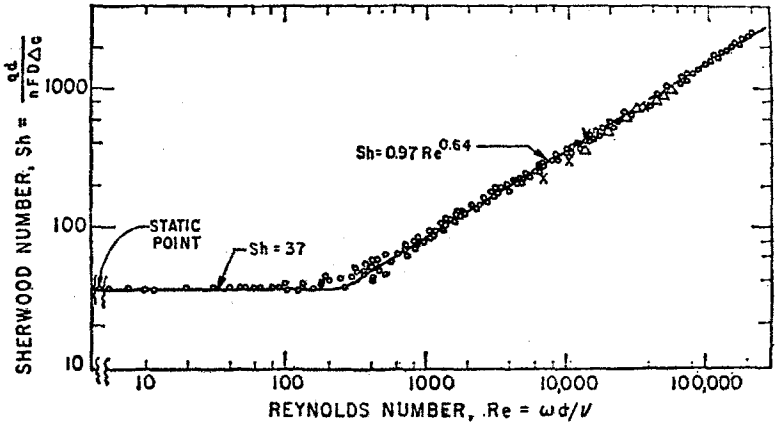

Fig. 10. The laminar-turbulent transition defined by mass transport data. After Cornet and Kappasser [81].

reported a transition in behaviour without being too explicit about the nature of that transition, and showed that for velocities below the critical velocity

$$i_L \propto R_1^{\frac{3}{4}}\, l^{\frac{3}{4}}\, \omega^{\frac{1}{2}} \tag{38}$$

Where R_1 and l were the radius and length respectively of the wire electrode. Above the critical velocity the relation was:

$$i_L \propto R_1^{\frac{2}{3}}\, l^{\frac{1}{3}}\, \omega^{\frac{1}{2}} \tag{39}$$

Doubt about the nature of this transition exists because Wilke *et al.* [88, 89] have reported that for free convection at vertical plate electrodes a correlation of the following form is found:

$$\mathrm{Sh} = 0{\cdot}66\ (\mathrm{Sc\ Gr})^{\frac{1}{4}} \tag{40}$$

where the Grashof number Gr may be thought to be analogous to the Reynolds number as a velocity term. A semi-rigorous theoretical approach to mass transfer in the laminar regime [90, 91] indicates that $i_L \propto \mathrm{Re}^{\frac{1}{2}}$ thereby suggesting that the critical velocity of Kambara *et al.* [87] in fact refers to a transition between free and laminar forced convection.

Some consideration has been given to incorporating a free convection term in the equation for mass transfer under forced convection although in practice it is a negligible contribution. Culbertson and Rutkowski [74] drew the analogy between mass and heat transfer in fluid flow but mistakenly analysed the redox reaction Ce^{3+}/Ce^{4+} in terms of the anodic current efficiency which increased from a finite static value under the influence of electrode rotation (0–5000 r.p.m.):

$$(\mathrm{ACE})_{\mathrm{rot}} = (\mathrm{ACE})_{\mathrm{stat}} + bU^{\frac{1}{2}} \tag{41}$$

For cementation of copper by iron, Rickard and Fuerstenau [76] determined the rate of deposition for 0–800 r.p.m. rotation speed as an equivalent current:

$$i = K_1 + K_2 U^{\frac{1}{2}}$$

In both these equations there is effectively a free and forced convective term. Analysis of the free convective term is primarily of interest to electroanalytical chemists and various treatments may be found [1, 92, 93]. The 'free convective' diffusion current at a cylindrical wire electrode, radius R_1, is often given as [1]:

$$i_d = zFADC_b \frac{1}{R_1}\left[\frac{1}{\pi^{\frac{1}{2}}\phi^{\frac{1}{2}}} + \tfrac{1}{2} - \tfrac{1}{4}\left(\frac{\phi}{\pi}\right)^{\frac{1}{2}} + \tfrac{1}{8}\phi\right] \tag{42}$$

where $\phi = Dt/R_1^2$ and t is the transient time of current decay after initial switching on. Various approximations may be made for this general equation depending upon conditions prevailing and when $R_1 = 0{\cdot}1$ cm and $t > 10$ s the first term only of the expansion may be adequate. Brown [94] gives a less specific approximation as:

$$I_d = 4\pi zFDC_b R_1\,[1 + R_1(\pi Dt)^{-\frac{1}{2}}] \tag{42a}$$

4.3. *Theoretical analysis*

The problem of deriving a mass transport

equation for the RCE is to a large extent a matter of defining a model and justifying the velocity/distance profile across the annular gap which is assumed. In laminar flow the velocity distribution equation is usually taken to be parabolic in form; approximation to a linear relation may be good near the rotating cylinder but less satisfactory nearer the static cylinder (see Fig. 3). For turbulent flow any single equation must necessarily be complicated and its range of applicability limited by the stability of flow as discussed earlier (Section 3).

4.3.1. *Laminar flow.* Three analyses of mass transport in laminar flow have been published [90, 91, 95], the two earliest of which assume a linear velocity profile β ($= U/y$) near the inner rotating cylinder and consider behaviour at a segment length M of the cylinder such that $M \ll 2\pi R_1$; the segment may be considered planar with a tangential velocity axis x. Implicit in the analysis is the assumption of non-rotational flow of the fluid. The later analysis of Mohr and Newman [95] treats steady state 'Couette' flow, where the fluid rotates under its own developed momentum, using a more complex velocity profile and makes allowance for surface curvature at the segment M.

Following the treatment of Gabe and Robinson [90] the boundary conditions at the inner cylinder radius R_1 are that $C = C_b$ as $y \to \infty$ and $C = C_s$ at $y = 0$. By using a dimensionless parameter $X = y\,(\beta/9Dx)^{\frac{1}{3}}$ the diffusion equation may be expressed as:

$$C - C_s = \frac{1}{0{\cdot}893} \int_0^X \exp(-X^3)\,dX \qquad (43)$$

The diffusion current density is defined as:

$$i_L = zFJ = zFD\left[\frac{dC}{dy}\right]_{y=0} \qquad (44)$$

By substituting and integrating the current for the whole surface M from 0 to $2\pi R_1$:

$$i_L = \frac{1}{M}\frac{zFD(C_b - C_s)}{0{\cdot}893}\left[\frac{\beta}{9D}\right]^{\frac{1}{3}} \int_0^M x^{-\frac{1}{3}}dx$$

$$= 0{\cdot}807\, zFD^{\frac{2}{3}}(C_b - C_s)M^{-\frac{1}{3}}\beta^{\frac{1}{3}} \qquad (45)$$

A velocity profile equation for the whole annulus $(R_2 - R_1)$ was taken from Levich [3] and Bird *et al.* [96] as:

$$U = \omega_1 R_1^2\left[\frac{1}{r} - \frac{r}{R_2^2}\right]\left[1 - \frac{R_1^2}{R_2^2}\right]^{-1} \qquad (46)$$

which on substitution for β over the whole gap yields:

$$i_L = 0{\cdot}807\, zFD^{\frac{2}{3}}(C_b - C_s)M^{-\frac{1}{3}}\omega^{\frac{1}{3}}\left[\frac{1 + R_1^2/R_2^2}{1 - R_1^2/R_2^2}\right]^{\frac{1}{3}} \qquad (47)$$

By using dimensionless groups this equation becomes:

$$\mathrm{Sh} = 0{\cdot}64\left[\mathrm{Re\,Sc}\,\frac{R_1}{M}\left\{\frac{1 + R_1^2/R_2^2}{1 - R_1^2/R_2^2}\right\}\right]^{\frac{1}{3}} \qquad (48)$$

If the whole cylindrical surface is used as electrode $M = 2\pi R_1$ and the length L should be included. Kimla and Strafelda [91] used a somewhat different velocity profile and obtained a value for the current on the segment:

$$I = 0{\cdot}48\, zFC_bLM^{\frac{2}{3}}D^{\frac{2}{3}}\omega_1^{\frac{1}{2}}(1 - R_1^2/R_2^2)^{-\frac{1}{3}} \qquad (49)$$

or

$$\mathrm{Sh} = 0{\cdot}38\left[\frac{\mathrm{Re\,Sc}}{(1 - R_1^2/R_2^2)}\frac{R_1}{M}\right]^{\frac{1}{3}} \qquad (50)$$

Comparison with Equations 47 and 48 shows that the geometrical factors and constant are different but the dependence of Sh on Re and Sc remains the same. This dependence has been verified by Ibl *et al.* [97] for a rotating wire but the results of Kambara *et al.* [87] and Cornet and Kappesser [81] are at some variance. These last authors correlated results for one solution at one temperature (Sc constant) and obtained a relation:

$$\mathrm{Sh} = f\,\mathrm{Re\,Sc}^{\frac{1}{3}} \qquad (37)$$

which for Sc = 460 and f = constant/Re gave a value of Sh = 37. Thus the experimental results apparently show that Sh is constant for the range $5 < \mathrm{Re} < 200$ suggesting that the fluid is probably rotating with the inner cylinder and therefore not contributing significantly to enhancement of the mass transfer rate (see Fig. 11).

Mohr and Newman [95] have attempted to

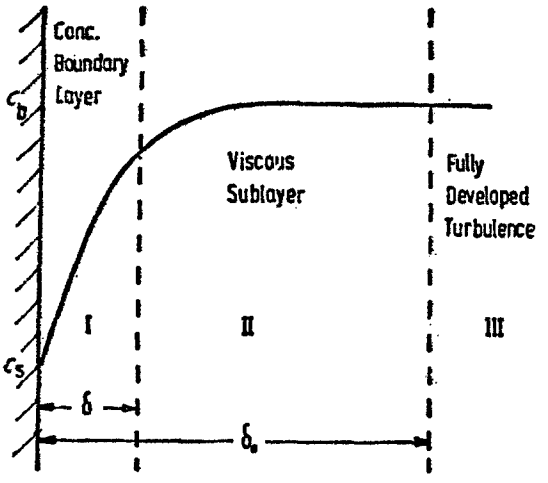

Fig. 11. Model of turbulent flow showing a concentration distribution over three zones [80].

treat this case and instead of using static cartesian co-ordinates used rotating cylindrical co-ordinates and incorporated corrections for ellipticity of the diffusion layer at leading and trailing edges of the segment, curvature of the electrode surface and non-linearity of the velocity profile. By using a similar approach to Gabe and Robinson, but making use of some special solutions obtained elsewhere by Newman, the mass transport equation was given as

$$\mathrm{Sh} = 1{\cdot}0174\ \mathrm{Pe}^{\frac{1}{3}}\left[1+0{\cdot}1966\left(\frac{L}{R_1}\right)\mathrm{Pe}^{-\frac{1}{3}} +0{\cdot}618\ \mathrm{Pe}^{-\frac{1}{2}}+\left\{0{\cdot}009949\left(\frac{L}{R_1}\right)^2 -0{\cdot}1548\right\}\mathrm{Pe}^{-\frac{2}{3}}+\ldots\right] \quad (51)$$

where the Peclet number $\mathrm{Pe} = \beta L^2/2D$

Comparison with Equations 48 and 50 shows that the first terms are essentially similar but thereafter the 'correction' terms are different. Mohr and Newman [95] point out that the higher order terms ought to be considered although the correction incurred represents at the most 6–7% error. However, more fundamentally, the treatment still does not account for the experimental value of Sh = 37 obtained by Cornet and Kappesser [81].

4.3.2. *Turbulent flow.* The case of turbulent flow has also been treated by Gabe and Robinson [80] who assumed a velocity profile illustrated in Fig. 3 and used a model based on the three-zone concept of Prandtl and van Karman (Fig. 11). An expression for the turbulent diffusion coefficient was obtained by assuming an 'apparent' eddy viscosity component in turbulent regimes whose values have been given by Diessler [98]. Thus for zone III:

$$D_{\mathrm{III}} = n^2 yU \arctan\left(a\frac{y}{R_1}\right) \quad (52)$$

where n and a are constant, and for zone II:

$$D_{\mathrm{II}} = n^2 yU\left[1-\exp\left(-\frac{n^2 yU}{\nu}\right)\right] \arctan\left(a\frac{y}{R_1}\right) \quad (53)$$

When $R_1 \gg y$ we can approximate this equation to

$$D_{\mathrm{II}} = \frac{by^3 U^2}{\nu R_1} \quad (54)$$

where b is a constant ($= an^4$). This equation is extrapolated to the I/II zone boundary and we may also use

$$C_{\mathrm{II}} = C_b + \frac{J\nu R_1}{2bU_1^2}\left[\frac{1}{\delta_0^2}-\frac{1}{y^2}\right] \quad (55)$$

Where δ_0 is the hydrodynamic boundary layer thickness and J is the mass transport flux. By applying Fick's law in zone I (the diffusion layer) we may obtain that

$$\delta = \left[\frac{D\nu R_1}{bU_1^2}\right]^{\frac{1}{3}} \quad (56)$$

and in terms of a current density

$$i = b^{\frac{1}{3}} zFU_1^{\frac{2}{3}} D^{\frac{2}{3}} \nu^{-\frac{1}{3}} R_1^{-\frac{1}{3}} (C_b - C_s) \quad (57)$$

Substituting $U_1 = \omega R_1$ and using dimensionless groups

$$\mathrm{St} = (2b)^{\frac{1}{3}}\mathrm{Re}^{-\frac{1}{3}}\mathrm{Sc}^{-\frac{2}{3}} \quad (58)$$

or

$$\mathrm{Sh} = (2b)^{\frac{1}{3}}\mathrm{Re}^{\frac{2}{3}}\mathrm{Sc}^{\frac{1}{3}} \quad (59)$$

This treatment cannot yield a value for the constant $(2b)^{\frac{1}{3}}$ which depends on cell geometry and particularly friction or drag caused by

roughness effects. However, using the relation of Theodorsen and Regier [45] as in Equation 26 the constant is found to be 0·079 and this has also been found experimentally [6, 7, 20, 79]. Cornet and Kappesser [81] have obtained a relation (at constant Sc = 460) of

$$Sh = 0{\cdot}97\ Re^{0{\cdot}64} \qquad (60)$$

Assuming a dependence of $Sc^{\frac{1}{3}}$ this yields a constant of 0·126 which is of the same order of magnitude. It may be noted that if such a dependence of Sc can be assumed Robinson and Gabe [23] obtained:

$$Sh = 0{\cdot}169\ Re^{0{\cdot}66}\ Sc^{0{\cdot}33} \qquad (61)$$

showing that in a data correlation small changes in indice may cause large changes in the empirical value of the constant.

The theoretical treatments described can at best be described as semi-rigorous and incorporate approximations and simplifications of what might be a very complex model. However, the agreement between the equations derived and the experimental correlations is good suggesting that the approach is probably correct and the model adequate for most purposes.

5. Applications of the RCE

5.1. *Electroanalysis*

The relation between the RCE and the RDE was considered in the introduction but in fact the RCE has found relatively little use in the field of electroanalysis. Adams [1] has reviewed this field and has emphasized that rotating wire electrodes do have a role. Although initiated by Nernst and Merriam [48] it was later workers who placed the RCE technique on a sound footing [87, 97, 99, 100] using a 0·5 mm platinum wire projecting 5–10 mm from the end of a rotating glass stirring rod. The normal mode is vertical; horizontal electrodes have been used but are less satisfactory because of inconvenience in mounting and porrer stability for convective flow [101]. The importance of a free convective diffusion term has been emphasized by Brown [94] who discusses applications in the determination of D and z for a diffusion-controlled electrode reaction.

The vertical platinum wire electrodes has also been used in a vibrating rather than rotating mode [1] and may be powered by the voice coil of a loudspeaker [102] at audio frequencies (20–10 000 Hz). Harris and Lindsey [103–105] have shown that at low frequencies (<40 Hz) the limiting c.d. is proportional to frequency but at higher values they are virtually independent. The case of a vertical wire electrode vibrating perpendicular to its axis has been considered by Grafov [106] who has attempted a dimensional analysis for this case.

5.2. *Electrodeposition*

Early work on electrodeposition has been reviewed by Narasimham and Udupa [18] and is essentially qualitative making use of the motion to increase rates of electrowinning and improve surface finish of protective plated coatings. The use of cathodic copper deposition as a reaction to study mass transfer at the RCE has already been described and some of this work has been extended to a discussion of electrodeposit structure and the incidence of diffusion-controlled nodular and dendritic growths [23, 107–109]. (In this application the presence of uniform current over a large area is of particular importance as extensive microscopical examination is required). This approach is important in the development of high-speed electrodeposition processes and the RCE has been used to simulate continuous strip coating processes [19, 22] and might well also be used for continuous wire coating processes [110–113].

One application likely to be of considerable importance in the future is the electrowinning of metals from waste effluent and dilute leach or pickle liquors. Surfleet and Crowle [114] have discussed the competitive position of the RCE in relation to other processes such as fluidized bed electrodes, annular and parallel plate electrode configurations, etc., the specific requirement being the ability to recover metal from increasingly dilute solutions. This application may not have been envisaged by Edwards and Wall [21], nevertheless their considerations of power consumption while using the rotating cylinder cell are of relevance in this context. The electrochemical approach to effluent treatment

has obvious attractions [115] but commercial processes are at present limited to zinc, tin, gold and silver [116] with other metals such as nickel and copper likely to be treated similarly in the very near future. One particular problem in this field is the need to electrodeposit at high efficiency from very dilute solutions; that this problem is not insuperable is clear from the commercial success of recovering silver from waste photographic solutions using the RCE [117] (300 such units are reported to be in operation in the U.K. alone [118] at the end of 1973).

5.3. *Cementation*

Agitation can only have a beneficial effect on a cementation-type of reaction when it is controlled by ion diffusion through solution. This has been found for a number of cases and both the RDE and RCE have been used [119, 120]. Much work has been reported for systems where the geometry is irregular and the degree of agitation uncertain and in some cases the RDE has been preferred owing to the independence of diffusion flux and position [119].

The RCE has been used by King and co-workers [65–67] and Ingraham and co-workers [71–73] to examine rates of cementation-displacement for a variety of metals. The speed of rotation must be carefully chosen to ensure that diffusion is rate-controlling because at higher speeds chemical reaction becomes controlling [65, 71], the critical speed varying from one chemical system to another. In most cases the rate of deposition increased with rotation speed but Von Hahn and Ingraham [71, 72] have described two alkaline cyanide solutions for silver-copper and silver-zinc where the rate of cementation is decreased by increased rotation speed. Strickland and Lawson [119, 120] have pointed out that there is a significant roughness effect in terms of increased surface area for reaction and this has not always been adequately considered.

5.4. *Corrosion and dissolution*

Much of the earlier work involving the RCE was carried out for corrosion reactions but because of the marked tendency for chemical reaction to become rate-controlling there is a fair amount of confusion in the literature. At low rotation speeds (<1000 r.p.m.) the rate of corrosion was found to depend upon $\omega^{0.7}$ while at speeds in excess of 500 r.p.m. it was often found to be independent of the speed [58–64, 68, 69]. At intermediate rotation speeds the power index was found to have values of 0·7–1·0 as partial control was exercised. Other factors were recognized; for example, Roald and Beck [56] found that at low acidity the rate of dissolution of magnesium in hydrochloric acid was proportional to $\omega^{0.71}$ but if the acidity was >1·4 M then were independent because of interference by the evolution of hydrogen bubbles.

The effects of solution flow on rates of corrosion have generally been examined by flow rigs but Heitz [121] has pointed out that disc and cylinders are much more convenient for laboratory testing. On this basis the RCE has been used to investigate effects of dissolved oxygen [122] and chlorides [123, 124] on rates of corrosion, efficacy of inhibitors in controlling corrosion [65] and cathodic protection in flowing conditions [68, 85]. Makrides [47, 77, 125] has attempted to introduce a roughness factor into the mass transport equation pointing out that a surface generally becomes rougher as dissolution takes place whereupon the rate becomes directly proportional to rotation speed.

Non-faradaic dissolution of benzoic and cinnamic acids was investigated by Eisenberg *et al.* [6, 7] and others [126] and recently Holman and Ashar [127] have attempted to distinguish between reacting and non-reacting dissolution in aqueous alkaline solutions containing glycerol. They obtained correlations of the type

$$\mathrm{Sh} = a\ \mathrm{Sc}^b\ \mathrm{Re}^c \qquad (62)$$

For non-reacting dissolution $a = 9{\cdot}3$, $b = 0{\cdot}33$, $c = 0{\cdot}425$ and for reacting dissolution $a = 88{\cdot}2$, $b = 0{\cdot}33$, $c = 0{\cdot}492$. The fact that the values of a and c depart so markedly from those found previously suggests that the dissolution was not completely diffusion-controlled and that as found elsewhere for alkaline solutions [71, 72] some other mechanism assumes importance—perhaps amphoteric complex formation.

More recently the RCE has been used to examine transport behaviour in liquid metals

and fused salts. For dissolution of metals in liquid metals the Eisenberg correlation has been used as a criterion for diffusion control in view of the marked departures observed [128–130], although in the case of carbon steel dissolving into a melt of an essentially similar alloy the departure was relatively small [131]. It is clear that in such applications complex solution chemistry involving solute-solute or solvent-solute interaction are much more likely to be rate-controlling. However, the analytical control of such processes by voltammetry at the RCE may well prove to be feasible as a continuous monitor [132].

References

[1] R. N. Adams, 'Electrochemistry at Solid Electrodes', Dekker, New York (1969).
[2] W. J. Albery and M. L. Hitchman, 'Ring-Disc Electrodes', O.U.P. (1971).
[3] V. G. Levich, 'Physiochemical Hydrodynamics', Prentice-Hall, New York (1962).
[4] J. Newman, 'Electrochemical Systems', Prentice-Hall, New York (1973).
[5] I. Cornet, W. N. Lewis and R. Kappesser, *Trans. Inst. Chem. Eng.*, **47** (1969) T222.
[6] M. Eisenberg, C. W. Tobias and C. R. Wilke, *J. Electrochem. Soc.*, **101** (1954) 306.
[7] *Idem, Amer. Inst. Chem. Eng. Sympos.*, Ser. no. 16, **51** (1954) 1.
[8] M. J. Lighthill, *Proc. Roy. Soc.*, **A202** (1950) 359; **A224** (1954) 1.
[9] B. W. Martin and A. Payne, *Proc. Roy. Soc.*, **A328** (1972) 123.
[10] A. C. Merrington, 'Viscometry', Arnold, London (1949).
[11] G. F. C. Searle, 'Experimental physics', Cambridge University Press (1934).
[12] T. Mizushina, 'Advances in Heat Transfer', Eds. Irvine and Hartnett, Acad. Press (1971), Vol. 7, 87.
[13] J. Postlethwaite and K. L. Ong, *Electrochim. Acta* **16** (1971) 661.
[14] E. Brunner, *Z. Phys. Chem.*, **47** (1904) 56; **51** (1905) 95; **58** (1907) 1.
[15] C. W. Bennett, *Trans. Electrochem. Soc.*, **21** (1912) 245.
[16] C. G. Fink and C. B. F. Young, *ibid.*, **67** (1935) 311.
[17] C. G. Fink and H. B. Linford, *ibid.*, **72** (1937) 461.
[18] K. C. Narasimhan and H. V. K. Udupa, *Met. Fin. J.*, **18** (1972) 11, 32.
[19] D. A. Swalheim, *Trans. Electrochem. Soc.*, **86** (1944) 395.
[20] A. J. Arvia and J. S. W. Carrozza, *Electrochim. Acta.*, **7** (1962) 65.
[21] J. Edwards and A. J. Wall, *Trans. Inst. Min. Met.*, **75** (1966) C307.
[22] L. R. Beard, D. R. Gabe and S. H. Melbourne, *Trans. Inst. Met. Fin.* **44** (1966) 1.
[23] D. J. Robinson and D. R. Gabe, *ibid.*, **48** (1970) 35.
[24] D. J. Robinson, Ph.D. Thesis, Univ. Sheffield (1970).
[25] R. Kappesser, I. Cornet and R. Greif, *J. Electrochem. Soc.*, **118** (1971) 1957.
[26] E. A. von Hahn and T. R. Ingraham, *Trans. A.I.M.E.*, **236** (1966) 1098.
[27] *Idem*, **239** (1967) 1895.
[28] A. R. Kuhltau, *J. Appl. Phys.*, **20** (1949) 217.
[29] R. A. Dimon, *Proc. Amer. Electropl. Soc.* **36** (1948) 169.
[30] R. Mills and C. J. Thwaites, *Sheet Met. Ind.*, **31** (1954) 733.
[31] B. T. K. Barry and C. J. Thwaites, *Metallurgia*, **74** (1966) 51; *Trans. Inst. Met. Fin.*, **44** (1966) 143.
[32] D. R. Gabe, Discussion of ref. [31] *Trans. Inst. Met. Fin.*, **44** (1966) 144.
[33] J. R. Rawlings and C. D. Costello, *J. Metals*, **21** (1969) 49.
[34] R. W. Bartlett, M. C. Van Hecke and C. Q. Hoard, *Met. Trans.*, **3** (1972) 2241.
[35] H. Starsinzky, K. Hein and D. Schab, *Neue Hutte*, **18** (1973) 346.
[36] A. Mallock, *Phil. Trans. Roy. Soc.*, **A187** (1896) 41.
[37] G. I. Taylor, *ibid.*, **A223** (1923) 289.
[38] *Idem, Proc. Roy. Soc.*, **A102** (1923) 541.
[39] *Idem*, **A157** (1936) 546.
[40] C. C. Lin, 'The Theory of Hydrodynamic Stability', Cambridge University Press (1955).
[41] J. R. Flower, N. Macleod and A. P. Shahbendarian, *Chem. Eng. Sci.* (1969) 637.
[42] H. Schlichting, 'Boundary Layer Theory', McGraw-Hill, New York, 6th ed. (1968).
[43] H. G. Jerrard, *J. Appl. Phys.*, **21** (1950) 1007.
[44] S. Chandrasekhar, *Proc. Roy. Soc.*, **A246** (1958) 301.
[45] T. Theodorsen and A. Regier, *Nat. Advisory Comm. Aeronaut.* (1945) rep. 793.
[46] R. J. Donnelly *et al.*, *Proc. Roy. Soc.*, **A246** (1958) 312; **A258** (1960) 101; **A281** (1964) 130; **A283** (1965) 509, 520, 531.
[47] A. C. Makrides and N. Hackerman, *J. Electrochem. Soc.* **105** (1958) 156.
[48] W. Nernst and E. S. Merriam, *Z. Phys. Chem.*, **53** (1905) 235.
[49] O. Sackus, *ibid.*, **54** (1906) 641.
[50] K. Jablczynski, *ibid.*, **64** (1908) 748.
[51] M. Wilderman, *ibid.*, **66** (1909) 445.
[52] R. G. Van Name and G. Edgar, *ibid.*, **73** (1901) 97; *J. Am. Chem. Soc.*, **28** (1910) 237.
[53] A. Eucken, *Z. Phys. Chem.*, **59** (1907) 72.
[54] *Idem, Z. Elektrochem.*, **38** (1932) 341.
[55] J. H. Jacob *et al.*, *Trans. Electrochem. Soc.*, **86** (1944) 383; **90** (1946) 211; **94** (1948) 108.
[56] B. Roald and W. Beck, *ibid.*, **98** (1951) 277.
[57] C. V. King, *ibid.*, **102** (1955) 193.
[58] C. V. King, *J. Am. Chem. Soc.*, **57** (1935) 828.
[59] C. V. King and M. Schack, *ibid.*, 1212.
[60] C. V. King and W. H. Cathkart, *ibid.*, **59** (1937) 63.
[61] C. V. King and P. L. Howard, *Ind. Eng. Chem.*, **29** (1937) 75.
[62] H. Salzberg and C. V. King, *J. Electrochem. Soc.*, **97** (1950) 290.
[63] C. V. King and F. S. Lang, *ibid.*, **99** (1952) 295.
[64] C. V. King and N. Mayer, *ibid.*, **100** (1953) 473.

[65] C. V. King and M. M. Burger, *ibid.*, **65** (1934) 403.
[66] M. B. Abramson and C. V. King, *J. Am. Chem. Soc.*, **61** (1939) 2290.
[67] R. Glicksman, H. Mouguin and C. V. King, *J. Electrochem. Soc.*, **100** (1953) 580.
[68] C. V. King and E. Hillner, *ibid.*, **101** (1954) 79.
[69] P. M. Christopher and C. V. King, *ibid.*, **107** (1960) 493.
[70] M. Centnerszwer and W. Heller, *Z. Phys. Chem.*, **A161** (1932) 113.
[71] E. A. Von Hahn and T. R. Ingraham, *Trans. A.I.M.E.*, **236** (1966) 1098.
[72] *Ibid.*, **239** (1967) 1895.
[73] T. R. Ingraham and R. Kerby, *ibid.*, **245** (1969) 17.
[74] J. L. Culbertson and C. Ritkowski, *Trans. Electrochem. Soc.*, **81** (1942) 185.
[75] J. L. Culbertson and W. C. Teach, *ibid.*, **81** (1942) 191.
[76] R. S. Rickard and M. C. Fuerstenau, *Trans. A.I.M.E.*, **242** (1968) 1487.
[77] A. C. Makrides, *Corrosion* **18** (1962) 338 t.
[78] J. Jordan, *Anal. Chem.* **27** (1955) 1708.
[79] D. R. Gabe and D. J. Robinson, *Trans. Inst. Met. Fin.* **49** (1971) 17.
[80] D. R. Gabe and D. J. Robinson, *Electrochim. Acta*, **17** (1972) 1129.
[81] I. Cornet and R. Kappesser, *Trans. Inst. Chem. Eng.*, **47** (1969) T 194.
[82] A. J. Arvia, J. S. W. Carrozza and S. L. Marchiano, *Electrochim. Acta*, **9** (1964) 1483.
[83] T. K. Sherwood and J. M. Ryan, *Chem. Eng. Sci.*, **11** (1959) 81.
[84] J. Postlethwaite and J. Sephton, *Corr. Sci.*, **10** (1970) 775.
[85] G. Kar, T. W. Healy and D. W. Fuerstenau, *ibid.*, **13** (1973) 375.
[84] J. Newman, *Ind. Eng. Chem.*, **60 (4)** (1968) 12.
[87] T. Kambara, T. Tsukamoto and I. Tachi, *J. Electrochem. Soc. Jap.* **18** (1950) 356, 386; **19** (1951) 199, 297.
[88] C. R. Wilke, M. Eisenberg and C. W. Tobias, *J. Electrochem. Soc.* **100** (1953) 513.
[89] *Idem, Chem. Eng. Prog.*, **49** (1953) 663.
[90] D. R. Gabe and D. J. Robinson, *Electrochim. Acta.*, **17** (1972) 1121.
[91] A. Kimla and F. Strafelda, *Coll. Czech. Chem. Comm.* **32** (1967) 56.
[92] M. Paunovic, *J. Electroanal. Chem.*, **14** (1967) 447.
[93] K. B Oldham, *ibid.*, **41** (1973) 351.
[94] O. R. Brown, *ibid.*, **34** (1972) 419.
[95] C. M. Mohr and J. Newman, *Electrochim. Acta*, **18** (1973) 761.
[96] R. B. Bird, W. E. Stewart and E. N. Lightfoot, 'Transport Phenomena', Wiley, New York (1960).
[97] N. Ibl, K. Buob and G. Trumpler, *Helv. Chim. Acta*, **37** (1954) 2251.
[98] R. G. Diessler, *Nat. Advisory Comm. Aeronaut* (1955) rep. 1210.
[99] H. A. Laitinen and I. M. Kolthoff, *J. Phys. Chem.*, **45** (1941) 1079.
[100] E. R. Nightengale, *Anal. Chim. Acta*, **16** (1957) 493.
[101] D. J. Ferrett and C. S. G. Phillips, *Trans. Faraday Soc.* **51** (1955) 390.
[102] E. R. Roberts and J. S. Meek, *Analyst* **77** (1952) 43.
[103] E. D. Harris and A. J. Lindsey, *Nature*, **162** (1948) 413.
[104] *Idem, Analyst* **76** (1951) 647, 650.
[105] A. J. Lindsey, *J. Phys. Chem.*, **56** (1952) 439.
[106] B. M. Grafov, *Soviet Electrochem.*, **3** (1967) 825.
[107] N. Ibl, *Adv. Electrochem. Eng.*, **2** (1962) 49.
[108] N. Ibl, G. Gut and M. Webber, *Electrochim. Acta*, **18** (1973) 307.
[109] D. R. Gabe, *Metallurgist* **5** (1973) 72.
[110] A. Tvarusko, *Plating* **58** (1971) 983.
[111] *Idem, J. Electrochem. Soc.* **119** (1972) 43.
[112] *Ibid.*, **120** (1973) 87.
[113] *Idem, Plating* **60** (1973) 345.
[114] B. Surfleet and V. A. Crowle, *Trans. Inst. Met. Fin.*, **50** (1972) 227.
[115] A. T. Kuhn, *Chem. and Ind.* **18** (1971) 473.
[116] R. Pinner, *Met. Fin. J.*, **13** (1967) 334; **19** (1973) 82.
[117] J. S. Bentley, Germ. Pat. 2044580 (1971); Brit. Pat. 1285602 (1972).
[118] *The Sunday Times*, 2 Dec., 1973, p. 32.
[119] P. H. Strickland and F. Lawson, *Proc. Austral. Inst. Min. Met.*, **236** (1970) 25.
[120] *Ibid.*, **237** (1971) 71.
[121] E. Heitz, *Werks. u Korr.* **15** (1964) 63.
[122] Z. A. Foroulis and H. H. Uhlig, *J. Electrochem. Soc.*, **111** (1964) 13.
[123] G. Butler and E. G. Stroud, *Brit. Corr. J.*, **1** (1965) 110.
[124] L. Giuliani, A. Tamba and C. Modena, *Inst. Corr. Sci.*, **11** (1971) 485.
[125] A. C. Makrides, *J. Electrochem. Soc.*, **107** (1960) 869.
[126] J. A. R. Bennett and J. B. Lewis, *J. Amer. Inst. Chem. Eng.*, **4** (1958) 485.
[127] K. L. Holman and S. T. Ashar, *Chem. Eng. Sci.*, **26** (1971) 1817.
[128] F. W. Hinzer and D. A. Stevenson, *J. Phys. Chem.*, **67** (1963) 2424.
[129] R. Ohno, *Met. Trans.*, **4** (1973) 909.
[130] H. Ooi, Y. Oguchi and H. Nakato, *Trans. Iron Steel Inst. Jap.*, **12** (1972) 1.
[131] M. Kosaka and S. Minowa, *Tetsu-to-Hagane*, **53**, (1967) 983.
[132] P. J. Bowles and D. G. Winter, 'Advances in Extractive Metallurgy', Inst. Min. Met., London (1971).